Aalborg Universitet

AALBORG UNIVERSITY
DENMARK

Data-Driven Controllability of Power Electronics Under Boundary Conditions

A Physics-Informed Neural Network Based Approach

Sahoo, Subham; Blaabjerg, Frede

Link to publication from Aalborg University

Data-Driven Controllability of Power Electronics Under Boundary Conditions – A Physics-Informed Neural Network Based Approach

Subham Sahoo, *Member, IEEE* and Frede Blaabjerg, *Fellow, IEEE*

Abstract—This paper introduces physics-informed neural network (PINN) for control of grid connected converter by fusing its underlying equations into the training process, thereby reducing the requirement of *qualitative* training data. In comparison to the traditional data-driven methods, which either incur a significant computational burden, or use overly conservative surrogate models, it is explored that PINN can be easily optimized as per the performance requirements and is significantly superior in terms of computation time, data requirements (trained using only 3000 datapoints), and prediction accuracy (an average of 98.76%). As a result, PINN unravels new modeling orientation for power electronics, and is well-suited for commercial applications. Finally, its robustness under various grid disturbances has been validated under experimental conditions.

Index Terms—Power electronics, Artificial intelligence, Physics-informed machine learning, Grid-tied inverter.

I. INTRODUCTION

Accurate modeling and control of grid-tied converters requires the evaluation of a large number of possible disturbances related to different active and reactive set-points under different voltage variations [1]. However, its behavior under boundary operating conditions introduces non-linearities, which makes it difficult to obtain an unified model. To tackle this issue, some traditional methods have been used [2], [3], which either carry a significant computational burden, require model simplifications, or use overly conservative surrogate models. Conventional neural networks (NNs) [4] can circumvent these limitations but are faced with high demand of high-quality training datasets, while they ignore the underlying governing equations. In addition, NNs suffer from lack of trust due to their black-box nature and them being agnostic to the well-studied physical models [5]. Yet, a high quality dataset can rarely be achieved from data collected from real-world systems. That is because the available real data is usually not enough and most importantly, it can not accommodate different non-linear events, as such events tend to be rare [6], [7].

To address these issues, physics-informed neural network (PINN) is used in this paper to generalize data-driven control of power electronics using minimal data without any compromise in precision. To provide a good balance of its estimation capabilities, the PINN training process is weighted
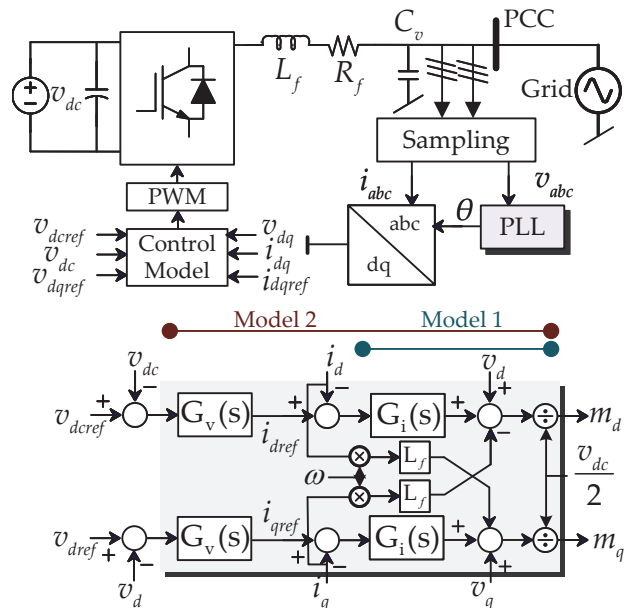
Fig. 1. Overall schematic of a grid-tied converter with its sampling circuit and control models `Model 1` and `Model 2`, which will serve as as the baseline models for training and design of NNs in this paper.

in accordance with the underlying physics and operational boundaries for control of grid-tied converters only using only 3000 datapoints with an average accuracy of 98.76%. Not only the computational burden is reduced, PINN facilitates an analytical representation and enhances the explainability of the conventional NNs.

II. DATA-DRIVEN ESTIMATION PROBLEMS UNDER BOUNDARY CONDITIONS

Considering a grid-following converter connected to strong grid (as shown in Fig. 1(a)), its dynamic equation in $dq0$ frame can be given by [9]:

$$\dot{\mathbf{x}} = \mathbf{A}\mathbf{x} + \mathbf{B}\mathbf{u} \qquad (1)$$

where, $\mathbf{x} = [i_d \ i_q \ v_d \ v_q \ v_{dc}]$, with the dq variables from measured AC voltages v_{abc}, AC currents i_{abc} and DC voltage v_{dc}, respectively. Furthermore, $\mathbf{u} = [v_{dref} \ v_{qref} \ v_{dcref}]$ denote a set of control inputs.

We now emphasize on the design of cascaded controllers for grid-tied converter. As shown in Fig. 1, `Model 1` ensures that

the current commands i_{dref} and i_{qref} are tracked simultaneously. To provide protection against overloading and external faults, the output of the compensators u_d, u_q in `Model 1` is limited by $[a_{min},a_{max}]$ for dq frame, respectively. The current-control scheme is designed based on the following dynamics:

$$L_f \frac{di_d}{dt} = -R_f i_d + u_d \tag{2}$$

$$L_f \frac{di_q}{dt} = -R_f i_q + u_q. \tag{3}$$

Upon decoupling and linearizing the `Model 1` output dynamics, we obtain:

$$m_d = \frac{2}{v_{dc}}(u_d - L_f \omega i_q + v_d) \tag{4}$$

$$m_q = \frac{2}{v_{dc}}(u_q + L_f \omega i_d + v_q). \tag{5}$$

Using the preliminary bounds of `Model 1`, we design its reference commands using `Model 2` (in Fig. 1) governing equations:

$$i_{dref} = G_v(s)(v_{dcref} - v_{dc}) \tag{6}$$

$$i_{qref} = G_v(s)(v_{dref} - v_d) \tag{7}$$

where, (8)-(9) are bounded by $[i_{min},i_{max}]$ in dq frame, respectively. As a result, the convoluted bounds in `Model 2` complicates the estimation problem under boundary conditions. The compensator outputs in `Model 1` & `Model 2` can attain values between finite range, which will lead it into roll over. Such undesirable condition can arise when the error is beyond particular limits, such as voltage sags, faults, large change in active/reactive power references. To limit the output, a saturation block can be used such that the new output can be expressed as:

$$y' = \begin{cases} y & \text{if } Y_{max} > y > Y_{min} \\ Y_{max} & \text{if } y > Y_{max} \\ Y_{min} & \text{else} \end{cases} \tag{8}$$

However, the limiting approach would lead to a convergence problem if the error remains non-zero for long and during that period the integrator output keeps on accumulating. As shown in Fig. 2, this either introduces delay in response when the input error changes or can even lead to roll over of the PI output.

As a result, some of the key challenges with the model-driven controllability for grid-tied converters are as follows:

1) Inaccurate estimation under boundary operating conditions;
2) Varying reactive power response as mandated by LVRT compliance requirements complicates the dynamic behavior.

This is where the trend has shifted towards data-driven controllability using neural networks (NNs), wherein the estimation is driven by the historic behavior and underlying dynamics based learning and approximation [8]. As shown in Fig. 3(b), the sampled data is collected and trained against non-linear activation functions for mapping the input-output relationship. However, the mapping accuracy is highly dependent on the
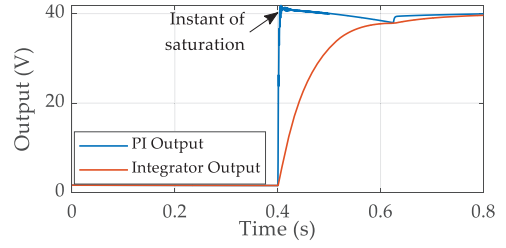

Fig. 2. Performance deviation between PI output and integrator output under boundary conditions – the problem aggravates under varying size of disturbances.
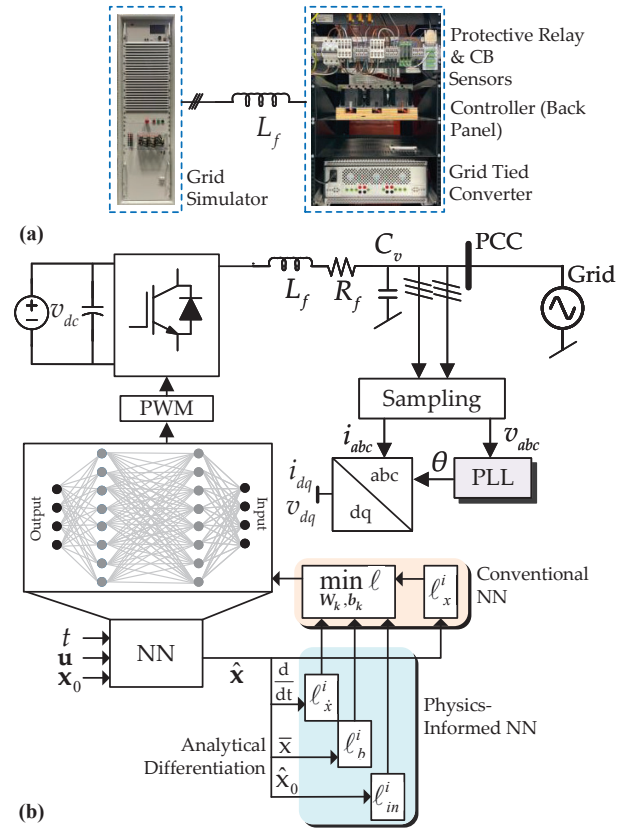
Fig. 3. (a) Experimental setup of the grid-tied inverter, (b) Overall schematic of the PINN based control strategy with new augmented terms for loss function of differential equation and boundary conditions of its predicted output.

quality of data. Data-driven estimation/regression accuracy has been largely attributed to the *quantity* of data, whereas it is prone to failure with absence of data representing particular operating conditions.

To ascertain the problem behind conventional NNs, the states **x** and inputs **u** dataset $\mathbb{D}_{3000001 \times 5}$ were obtained from a 2-level grid-tied converter of 10 kVA (as shown in Fig. 3(a)) to design a multi-layer feedforward NN with N_k hidden layers and N_L neurons per layer as a function approximator. The conventional NN (highlighted in Fig. 3(b)) using the defined

variables in $\mathbf{x}$ and $\mathbf{u}$ can be formulated by:

$$[t, \mathbf{x}_0, \mathbf{u}] = \mathbf{z}_0 \qquad (9)$$

$$\mathbf{z}_{k+1} = \phi(\mathbf{W}_{k+1}\mathbf{z}_k + \mathbf{b}_k) \ \forall \ k = 0, 1, \ldots, K-1 \qquad (10)$$

$$\hat{\mathbf{x}} = \mathbf{W}_{k+1}\mathbf{z}_k + b_{k+1} \qquad (11)$$

where, $\mathbf{W}_k$ and $\mathbf{b}_k$ denote the set of weights and biases in the kth layer. Basically, these weights are updated in every iteration by minimizing the loss $\mathcal{L}_x^i = \frac{1}{N_x}\sum_{j=1}^{N_x}(x_j^i - \hat{x}_j^i)$ in a supervised manner. Upon evaluating this loss separately for each dynamic state (indicated by superscript i), the training process is formalized by:

$$\min_{\mathbf{W},\mathbf{b}} \ \sum_i \lambda_x^i \mathcal{L}_x^i \qquad (12)$$

subject to (9)-(11), where λ_x^i provides weighting of the loss terms. However, even in a large dataset with numerous set-points in $\mathbb{D}$, it can be seen in Fig. 4 that conventional NNs fail to estimate accurately during boundary conditions. In Fig. 4(a), when the active power reference is changed from 0.6 pu to 0.65 pu at t = 0.08 sec, the system goes unstable with high frequency oscillations in the modulation index m_{dq}. A similar performance can also be seen initially in Fig. 4(b) where the dataset is reduced to $\mathbb{D}_{2500001 \times 5}$. However, due to reduced data as compared to the case studied in Fig. 4(a), a clear setback in performance can be observed in Fig. 4(b), where the system goes out of synchrony after t = 0.15 sec. Hence, the *quality* of data plays an important role in orchestrating conventional NN's performance, which anyway remains computationally expensive. In fact, the idea of using NNs to solve PDEs is not new and can date back to the last century [10]. These early works rely on the function approximation capabilities of a feedforward fully-connected neural networks to solve initial/boundary value problems. The solution to the system of equations can be obtained through minimization of the network's loss function, which typically consists of the residual error of the governing equations along with initial/boundary values. More recently, Raissi et al. [11], [12] has inherited and extended this concept, leveraged the strong expressibility of NNs, and developed the general physics-informed neural network (PINN) framework to solve the forward and inverse problems involving the system of nonlinear PDEs with small datasets or even without any labeled data. Furthermore, authors in [13] have also concluded that the global approximations can be easily calculated using the knot theory using physics-informed spline learning strategy for cybersecurity investigation in power electronics.

III. PHYSICS-INFORMED NEURAL NETWORK FOR POWER ELECTRONICS

A. Design of PINN

To address the inefficacy of conventional NNs in Section II, a physics-informed neural network (PINN) is designed to enforce that the updates from governing differential equations matches the temporal derivative of the NN's approximation $\frac{d}{dt}\hat{\mathbf{x}}$. $\frac{d}{dt}\hat{\mathbf{x}}$ is calculated by applying automatic differentiation (AD) [14] on the NN's output $\hat{\mathbf{x}}$ with respect to time to yield a new loss term $\mathcal{L}_{\dot{x}}^i$. Considering the dynamic equations of i_{dq}

from the current control scheme, we validate the NN output $\hat{i}_{dq}$ for Model 1 using AD of:

$$L_f \frac{d\hat{i}_d}{dt} = -R_f \hat{i}_d + L_f \omega \hat{i}_q + \frac{v_{dc}}{2}m_d - v_d \qquad (13)$$

$$L_f \frac{d\hat{i}_q}{dt} = -R_f \hat{i}_q - L_f \omega \hat{i}_d + \frac{v_{dc}}{2}m_q - v_q \qquad (14)$$

Similarly, the dynamics of other states in (1) can be validated using DC capacitor, line and load dynamics to apprehend the governing equations of Model 2 [9]. Finally, its estimation abilities are also enhanced by introducing another loss term to account a bounded optimization behavior of the NNs using another loss term $\mathcal{L}_b^i$. Finally, these loss terms are added to provide with the overall loss function (as highlighted in Fig. 3(b)), which can then be trained using:

$$\min_{\mathbf{W},\mathbf{b}} \ \sum_i \lambda_x^i \mathcal{L}_x^i \ + \ \lambda_{\dot{x}}^i \underbrace{\frac{1}{N_x}\sum_{j=1}^{N_x}(f^i(t_j, \mathbf{x}_j, \mathbf{u}_j) - \frac{d}{dt}\hat{x}_j^i)^2}_{\mathcal{L}_{\dot{x}}^i} \quad (15)$$

$$+ \ \lambda_b^i \underbrace{\frac{1}{N_x}\sum_{j=1}^{N_x}(f^i(t_j, \mathbf{x}_j, \mathbf{u}_j) - \bar{x}_j^i)^2}_{\mathcal{L}_b^i}$$

$$+ \ \lambda_{in}^i \underbrace{\frac{1}{N_x}\sum_{j=1}^{N_x}(f^i(t_j, \mathbf{x}_j, \mathbf{u}_j) - x_{j_{in}}^i)^2}_{\mathcal{L}_{in}^i}$$

subject to (9)-(11), where $\bar{x}_j^i$ and $x_{j_{in}}^i$ denote the boundary and initial condition of the corresponding states, respectively. The intuition behind (15) is that the prediction of the NN output $\hat{x}$ and its derivative $\frac{d}{dt}\hat{x}$ can be probed if they are consistent with the governing equations and can be optimized within the defined boundaries $\bar{x}$.

B. Generalization of PINN under boundary conditions

PINN reinforces design of a new approach with *qualitative* data, which would comply replacement of the existing model-driven/NN deployed in the system. This will not only incur increase in the replacement cost, but will also add uncertainty. In this paper, we also generalize the design process of PINN on a pre-trained NN structure by convoluting the distance parameter function based NN to make the overall control structure more robust to any given initial or boundary condition in the spatiotemporal space.

As shown in Fig. 6, an distance function based NN is deployed on top of the general pre-trained NN by convoluting it to structure the estimated output accordingly. This mechanism can be used to augment the general NN (which is not pre-trained using initial/boundary conditions data) with trained data properties that confer to only initial/boundary conditions. Finally to improve the overall performance, the weights $\mathbf{W}_k$ and biases $\mathbf{b}_k$ are optimized using automatic differentiation via governing equations of grid-tied converter, as shown in Fig. 6. The essence behind newly constructed solution is that, at the initial time or boundaries where the distance function evaluates
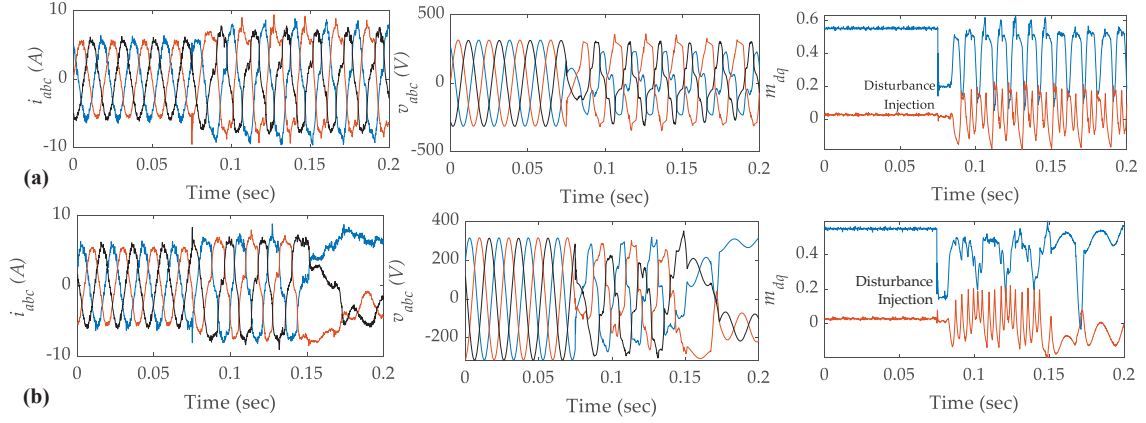
Fig. 4. Inefficacy of conventional NNs to provide good prediction under boundary conditions of i_{abc} without enough data leading to: (a) high frequency oscillations for the dataset with $\mathbb{D}_{3000001 \times 5}$ setpoints, (b) asynchrony after t = 0.15 sec for reduced setpoints in the dataset $\mathbb{D}_{2500001 \times 6}$.
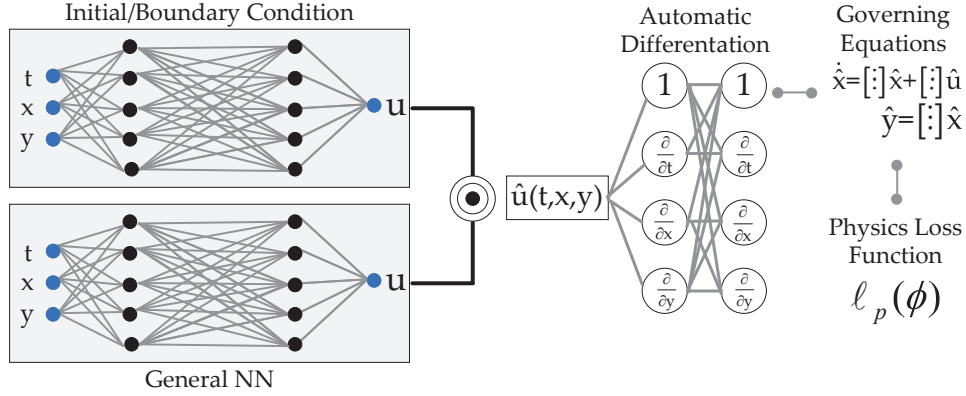

Fig. 5. Generalization of PINN design for *plug and play augmentation* into a pre-trained NN for hardly enforced initial/boundary conditions.
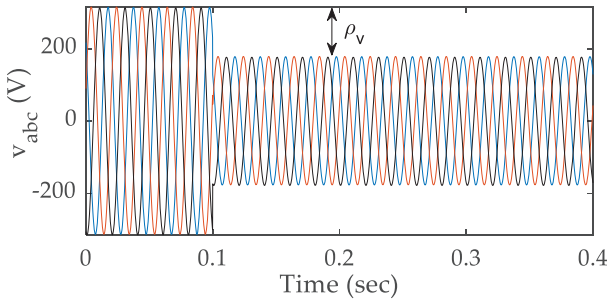

Fig. 6. Generalization of PINN by augmenting a pre-trained NN with a distance function based NN to accelerate its performance particularly around boundary conditions – this can be a *plug-and-play* approach of handling complex dynamics around boundary conditions for a pre-trained NN missing that capability.
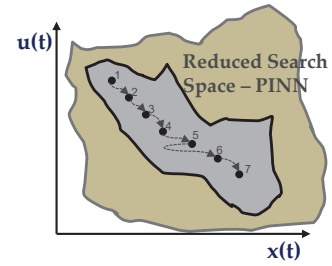

Fig. 7. PINN inherently incurs reduction in the dimensionality of dataset and computation burden, as the reduced search space is considerably small in comparison with the conventional NN due to underlying governing equations.

to zero, the solution degrades to the particular solution so that the boundary conditions will be imposed forcibly. This type of *hard* initial/boundary condition enforcement strategy can be generalized as follows:

$$\hat{\mathbf{u}}(\mathbf{x}, t) = \mathcal{D}(\mathbf{x}, t) \odot \mathbf{u}_p(\mathbf{x}, t) \qquad (16)$$

where, $\hat{\mathbf{u}}(\circ)$ denotes the final estimated output, $\mathcal{D}$ being the distance function and $\mathbf{u}_p(\circ)$ denotes the estimated output of the pre-trained NN. Furthermore, $\odot$ denote element-wise multiplication. To train the distance function $\mathcal{D}(\mathbf{x}, t)$, we can sample the points $(\mathbf{x}_i, t_i)_{i=1}^n$ and compute the distance $\mathcal{D}$ to the spatiotemporal boundaries for voltages and reactive power, shown as follows:

$$\begin{cases} \mathcal{D}_v = \min(\text{distance to the spatiotemporal boundary } \rho_v) \\ \mathcal{D}_Q = \min(\text{distance to the spatiotemporal boundary } \rho_Q) \end{cases} \qquad (17)$$

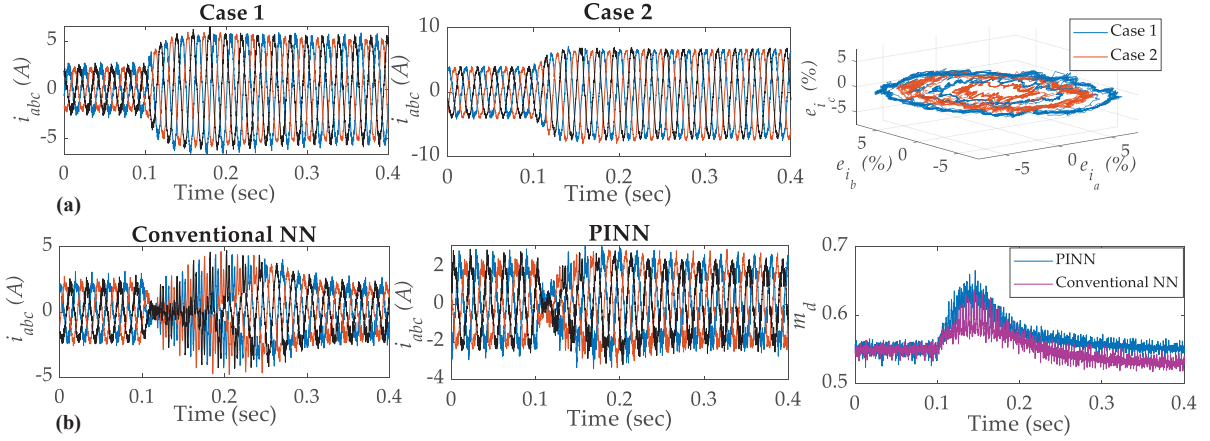where, ρ_v & ρ_Q denote the distance element between the

Fig. 8. (a) Performance of PINN for a light dataset $\mathbb{D}_{3000\times5}$ − Case 2 with equal weighting policies provide a better harmonic performance than Case 1 with a lower value of $\lambda_{\dot{x}}^i$, (b) Comparative evaluation of PINN with a dataset $\mathbb{D}_{3000\times5}$ against a conventional NN with a dataset $\mathbb{D}_{3000001\times5}$ − the dynamic performance is clearly better in PINN with a smaller settling time and overshoot.

boundary and measured value of voltages and reactive power, respectively. After $\mathcal{D}(x,t)$ is pre-trained and fixed, the composite PINN in Fig. 5 will be finally trained as a whole to make sure the remaining constraint, residual of governing PDEs, is satisfied. In the final training of the composite PINN, only the weights and biases of $\mathbf{u}_p(\mathbf{x},t)$ will be the trainable variables exposed to the optimizer.

As a result, the computation time and resources are significantly reduced owing to the fact that the search space is optimized particularly (as shown in Fig. 7) for the uncertain parameters with the rest assisted by the physics governed equations. It can be seen in Fig. 7 that the search plane is only a limited portion of the region generated for conventional NN.

C. Data collection policy

The major challenge behind designing an high fidelity PINN is on collection of *qualitative* data. Although we discuss about the generalization of PINN and enforce plug-and-play augmentation into a pre-trained PINN, the desired performance will only be possible provided significant data reflecting the spectral properties around initial/boundary conditions are obtained. Hence, we provide a state-dependent threshold based data collection policy, which saves data when:

$$||\rho_v|| > \beta||\rho_Q|| \quad (18)$$

is satisfied. It should be noted that β denote the LVRT gain as per the LVRT compliances and regulations [15]. More theoretical details about sampling and performance with different noise levels will be covered as a future scope of work.

IV. RESULTS

In Fig. 8, the performance of PINN for a dataset $\mathbb{D}_{3000\times5}$ is verified on the system shown in Fig. 3. It should be noted that the disturbances considered for the dataset of conventional NN remains uniform for a legitimate comparison. It can be seen in Fig. 8(a) for Case 1 that the PINN estimation still contains high frequency ripples in the current waveform, which necessitate prioritization of scaling of $\lambda_{\dot{x}}^i$ in (15). Finally, when
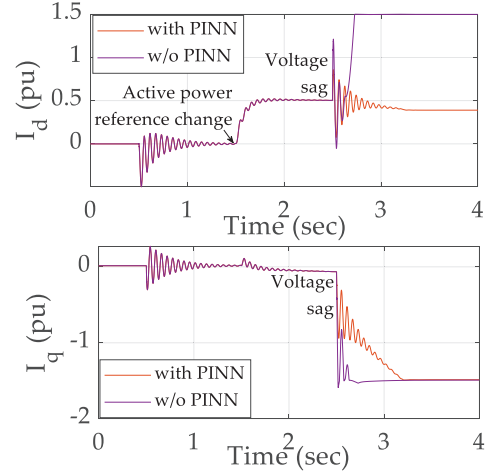

Fig. 9. Performance of PINN under a voltage sag of 0.6 p.u. at t = 2.5 sec − without PINN, the active power component increases invariably to the boundary condition, whereas PINN keep I_d restricted as per the LVRT regulations [15].

the weights are scaled equally in (15), it can be seen in Fig. 8(a) for Case 2 that the performance of PINN deems better tracking and dynamic performance than Case 1. The error plots plotted with respect to the corresponding reference values also clarify that the error (in %) is significantly lower for Case 2 than Case 1, which establishes new weight scaling policies to optimize PINN for power electronic converters. A comparative evaluation of PINN with a dataset $\mathbb{D}_{3000\times5}$ is carried out against a conventional NN with a dataset $\mathbb{D}_{3000001\times5}$ in Fig. 8(b). It can be seen that due to the additional loss functions $\mathcal{L}_{\dot{x}}^i$ and $\mathcal{L}_b^i$ in (15), better dynamic performance can be formally guaranteed with low settling time and overshoot for the proposed PINN scheme.

In Fig. 9, a comparative evaluation is carried out with and without PINN under a grid voltage sag of 0.6 p.u. at t = 2.5 sec. As per the established problem in Section II,

general PINN fails to estimate its operation around boundary conditions subject to the mandatory reactive power injection as per the regulations. This can be explained owing to the lack of *qualitative* training data around such boundary conditions. Furthermore without PINN, I_d saturates to the maximum active power injection capability, which compromises the ride-through operation and protection settings of grid-connected converter. However, when PINN is deployed as per the design policy shown in Fig. 5, the active component I_d is well restricted with the pre-fault operation point under boundary conditions. As a result, the proposed optimization process of NNs using PINN can not only reduce the dimensionality of data using the proposed data collection policy but also advances on highly cognitive and computationally efficient learning abilities of NNs under boundary conditions.

V. CONCLUSIONS AND FUTURE SCOPE OF WORK

This paper proposes a physics-informed neural network (PINN) based control of grid-tied converters for the first time only using minimal data of 3000 setpoints with an average accuracy of 98.76%. In this work, it has been shown that the usage of the governing physical equations fundamentally changes the workflow of applying NNs. Apart from obtaining a data-efficient training process, PINNs also offer the upside of providing easily computable metrics to identify areas of inaccuracy based on the agreement of the prediction with the physical equations. As a future scope of work, optimal sclaing policies of PINN weights in (15) with more theoretical analysis on its stability evaluation will be provided.

Appendix

An experimental prototype (as shown in Fig. 3) of two-level three-phase grid-tied converter of 10 kVA is connected to the grid simulator via an interfacing filter L_f.
System: L_f= 1.5 mH, R_f = 0.3 Ω, V_n = 230 V/50 Hz, f_{sw} = 10 kHz
PINN: $\lambda_{\dot{x}}^i = \lambda_x^i = \lambda_b^i = 0.4$, training dataset $\mathbb{D}_{3000 \times 5}$ setpoints with a sampling rate of 10 kHz.

REFERENCES

[1] S. Zhao, F. Blaabjerg, and H. Wang, "An overview of artificial intelligence applications for power electronics," *IEEE Trans. Power Electron.*, vol. 36, no. 4, pp. 4633-4658, 2020.

[2] M. G. Taul, X. Wang, P. Davari, & F. Blaabjerg, "Reduced-order and aggregated modeling of large-signal synchronization stability for multiconverter systems," *IEEE Journ. Emerg. Sel. Topics Power Electron.*, vol. 9, no. 3, pp. 3150-3165, 2020.

[3] Y. Pannatier, B. Kawkabani, C. Nicolet, J. J. Simond, A. Schwery, & P. Allenbach, "Investigation of control strategies for variable-speed pump-turbine units by using a simplified model of the converters," *IEEE Trans. Ind. Electron.*, vol. 57, no.9, pp. 3039-3049, 2009.

[4] X. Fu, S. Li, & T. Jaithwa, "Implement optimal vector control for LCL-filter-based grid-connected converters by using recurrent neural networks," *IEEE Trans. Ind. Electron.*, vol. 62, no. 7, pp. 4443-4454, 2015.

[5] C. Huang, J. Fan, W. Li, X. Chen, & Q. Zhu, "Reachnn: Reachability analysis of neural-network controlled systems," *ACM Trans. Embedded Computing Systems (TECS)*, vol. 18, no. 5s, pp. 1-22, 2019.

[6] S. Sahoo, H. Wang and F. Blaabjerg, "On the Explainability of Black Box Data-Driven Controllers for Power Electronic Converters," *2021 IEEE Energy Conversion Congress and Exposition (ECCE)*, pp. 1366-1372, 2021.

[7] A. Beattie, P. Mulinka, S. Sahoo, I. Christou, C. Kalalas, D. Gutierrez-Rojas & P. Nardelli, "A Robust and Explainable Data-Driven Anomaly Detection Approach For Power Electronics", *arXiv preprint arXiv:2209.11427*, 2022.

[8] B. K. Bose, "Neural network applications in power electronics and motor drives – An introduction and perspective" *IEEE Trans. Ind. Electron.*, vol. 54, no. 1, pp. 14-33, 2007.

[9] A. Yazdani, P. P. Dash, "A Control Methodology and Characterization of Dynamics for a Photovoltaic (PV) System Interfaced With a Distribution Network," *IEEE Trans. Power Delivery*, vol. 24, no. 3, pp. 1538-1551, 2209

[10] H. Lee, I. S. Kang, "Neural algorithm for solving differential equations," *Journ. Comp. Phys.*, vol. 91, no. 1, pp. 110-131, 1990.

[11] M. Raissi, P. Perdikaris, G. E. Karniadakis, "Physics-informed neural networks: A deep learning framework for solving forward and inverse problems involving nonlinear partial differential equations," *Journ. Comp. Phys.*, vol. 378, pp. 686-707, 2019.

[12] M. Raissi, Z. Wang, M. S. Triantafyllou, G. E. Karniadakis, "Deep learning of vortex-induced vibrations," *Journ. Fluid Mechan.*, vo. 861, pp. 119-137, 2019.

[13] V. S. B. Kurukuru, M. A. Khan and S. Sahoo, "Cybersecurity in Power Electronics Using Minimal Data – A Physics-Informed Spline Learning Approach," *IEEE Trans. Power Electron.*, vol. 37, no. 11, pp. 12938-12943, Nov. 2022.

[14] A. G. Baydin, B. A. Pearlmutter, A. A. Radul, and J. M. Siskind, "Automatic Differentiation in Machine Learning: a Survey," *Journal of Machine Learning Research*, vol. 18, no. 153, pp. 1-43, 2018.

[15] H. Geng, C. Liu, & G. Yang, "LVRT capability of DFIG-based WECS under asymmetrical grid fault condition" *IEEE Trans. Ind. Electron.*, vol. 60, no. 6, pp. 2495-2509, 2012.